Theory of plasmons in quasi-one-dimensional degenerate plasmas

M. Bonitz,* R. Binder, and D. C. Scott
Optical Sciences Center and Physics Department, University of Arizona, Tucson, Arizona 85721

S. W. Koch
Fachbereich Physik und Zentrum für Materialwissenschaften, Philipps Universität Marburg, Mainzergasse 33, 35032 Marburg, Germany

D. Kremp
Fachbereich Physik, Universität Rostock, Universitätsplatz 3, 18051 Rostock, Germany
(Received 5 August 1993)

An analysis of collective longitudinal electrostatic plasma excitations in quasi-one-dimensional degenerate plasmas is presented using the dielectric function in the random phase approximation. Analytical continuation of the dielectric function into the lower energy half plane allows us to compute the complete spectrum of the collective excitations, including frequencies and damping or growth rates. In contrast to two- and three-dimensional plasmas, a multicomponent quasi-one-dimensional system at zero temperature is found to exhibit one undamped plasmon mode for each component. The conditions for the occurrence of unstable modes are investigated and the influence of temperature and collisions on the results is discussed.

PACS number(s): 52.35.Fp, 73.20.Dx, 52.35.Qz, 71.45.Gm

I. INTRODUCTION

The experimental and theoretical study of nonideal plasmas is an area of substantial current interest [1]. Deviations from the ideal behavior dominate the plasma properties in a certain region of the density-temperature plane [2,3] (the so-called corner of correlations). Situations where strong correlations are present (i.e., where the Coulomb interaction between the carriers is not small compared to their kinetic energy) are encountered for low temperatures and/or high pressures. These conditions can be realized in freezing experiments on ionized gases, in astrophysical objects (e.g., inner layers of the giant planets), or ion-beam and laser compression experiments. Here, many-particle effects, such as degeneracy, screening, self-energy, bound states, lowering of ionization energy, and Pauli blocking have to be taken into account. The consequences of this include changes in both the thermodynamic and, more importantly, the nonequilibrium (transport) properties [4].

Collective excitations, which are another type of many-body behavior exhibited by plasmas, are of particular importance in nonequilibrium situations, because they can lead to instabilities and turbulence. Since the pioneering work of Vlasov and Landau [5–7] the questions of plasmons and instabilities have been extensively studied [8–11]. The Vlasov dielectric function is the appropriate starting point for an analysis of high-temperature gaseous plasmas as well as for low density plasmas (like in the atmosphere of the earth). It can also be used to study long wavelength excitations in solid-state plasmas. However, analyzing plasma instabilities using the Vlasov dielectric function restricts one to almost ideal and nondegenerate plasmas.

Traditionally, plasmons in degenerate charged-particle systems have been investigated only rarely in plasma physics ([12,13] and also [2], and references therein). After the pioneering work of Bohm, Pines, and Schrieffer [14,15] collective excitations in quantum plasmas have been primarily the subject of solid-state physics. However, most of these studies focused on the equilibrium situation. Only a considerably smaller number of papers has been devoted to nonequilibrium properties of quantum plasmas, focusing mainly on the problem of negative resistance [16]. Investigations of plasmon dispersions in nonequilibrium degenerate two-dimensional (2D) and 3D plasmas have been carried out recently [17]. In a number of papers Bakshi, Kempa, and co-workers systematically investigated the possibility of current-driven instabilities in a variety of layered solid-state systems (e.g., [18,19]). In a previous publication [20] we reported on the plasmon excitations in equilibrium and nonequilibrium quasi-1D quantum systems including the possibility of a carrier-acoustic instability, which was predicted also in [21] and further investigated in [19]. A 1D model is reasonable for quantum wires, narrow metal wires, and some types of conducting organic chains ([22–24], for reviews see, e.g., [25]). Moreover, many situations in plasma physics (e.g., homogeneous 3D plasmas) can be described by 1D models (after integrating the distribution function over the momentum components perpendicular to the excitation). In the rapidly growing field of electron-hole plasmas in semiconductor quantum wires,

*Permanent address: Universität Rostock, Fachbereich Physik, Universitätsplatz 3, 18051 Rostock, Germany.

low-temperature equilibrium plasmon spectra have been intensively investigated experimentally [26–28] and theoretically [29–33].

In the present paper we present more details of the previous calculations [20] and extend them to more general nonequilibrium situations. In order to point out the particular properties of collective excitations in quantum systems we compare our results to those for classical systems. Therefore we first summarize a few relevant results of the theory of Vlasov and Landau concerning longitudinal plasma oscillations in unmagnetized plasmas and discuss the theory's limitations (Sec. II). In the third section we derive the plasmon dispersion relation for 1D quantum plasmas by analytically continuing the retarded dielectric function (DF) within the random-phase approximation (RPA). We then calculate the plasmon dispersion for one- and two-component plasmas in equilibrium (Secs. IV and V, respectively), and for several nonequilibrium situations (Sec. VI). Finally we discuss the limitations of the RPA polarization (Sec. VII). By studying the influence of collisions on the plasmon spectrum within the Mermin approximation [34] we show that these effects are small in 1D. In order to check the validity of our analytic results we solve the nonlinear collisionless Boltzmann equation (Hartree equation) numerically. We show that for small amplitude plasma oscillations the RPA results agree very well with the solutions of the nonlinear kinetic equation.

II. VLASOV-LANDAU THEORY OF LONGITUDINAL ELECTROSTATIC PLASMA OSCILLATIONS

The longitudinal electrostatic plasmon spectrum is derived from the Vlasov equation [6] which yields, after linearization, the following complex DF of a 1D plasma:

$$\epsilon(\omega,\gamma,q)=1-\sum_a \frac{\omega_{pa}^2}{q^2}\,2\int_{-\infty}^{\infty} dv \frac{q df_a(v)/dv}{qv-(\omega-i\gamma)} , \quad (1)$$

where the index a denotes the charged-particle species. ω and γ denote, respectively, the real part and the negative of the imaginary part of the frequency ($\hat{\omega}=\omega-i\gamma$). We used the normalization $2\int f_a(v)dv=1$. ω_{pa} is the plasma frequency, cf. Eq. (3). The DF can also be written in the form

$$\epsilon(\omega,\gamma,q)=1-\sum_a V_a(q)\Pi_a(\omega,\gamma,q) . \quad (2)$$

Here, $V_a(q)=\omega_{pa}^2 m_a/q^2 n_a$ is the Fourier transform of the Coulomb potential. $\Pi_a(\omega,\gamma,q)$ is the polarization function [essentially the integral in Eq. (1)].

The plasmon dispersion follows from the condition $\epsilon(\omega,\gamma,q)=0$. An important advantage of the Vlasov dispersion is that one may treat a many-component plasma like an effective one-component system. The sum over the integrals in Eq. (1) can be reduced to one integral by introducing an effective (velocity dependent) distribution function $F(u)$ with a new plasma frequency ω_p,

$$\omega_p^2 F(u)=\sum_a \omega_{pa}^2 f_a(u) , \quad \omega_{pa}^2=4\pi e^2 n_a/m_a . \quad (3)$$

As we shall see below this is not possible for degenerate plasmas.

In order to highlight the main differences between the Vlasov and RPA dispersion we calculate the 1D Vlasov DF at $T=0$ K. To be as general as possible it is useful to consider the one-dimensional model distribution function [10]

$$F(u)=\sum_i A_i\Theta(u_{2i}-u)\Theta(u-u_{1i}) \quad (4)$$

for $u>0$ and for $u<0$, $F(-u)=F(u)$. Here, $0\le u_{1i}<u_{2i}$ and Θ denotes the Heaviside step function. We will consider the cases of (i) a one-component equilibrium plasma, (ii) a two-component equilibrium plasma, and (iii) a one-component nonequilibrium plasma. Distribution function (4) has the advantage that it can well approximate real distributions and at the same time allows us to find the plasmon spectrum analytically. For the polarization function, the integral in Eq. (1), we obtain

$$\mathrm{Re}\Pi(q,\omega)=\frac{2nq^2}{m}\sum_i A_i\left[\frac{2u_{2i}}{\omega^2-q^2u_{2i}^2}-\frac{2u_{1i}}{\omega^2-q^2u_{1i}^2}\right] , \quad (5)$$

$$\mathrm{Im}\Pi(q,\omega)=\frac{2\pi nq}{m}\sum_i A_i[\delta(\omega-qu_{1i})-\delta(\omega-qu_{2i})] . \quad (6)$$

(i) For a one-component plasma at $T=0$ K we set $i=1$, $u_1=0$, $u_2=u_F$ (Fermi velocity), and $A=1/4u_F$. In this case $\mathrm{Re}(\epsilon)$ as a function of ω has only one zero (at positive frequencies)

$$\Omega(q)=\sqrt{\omega_p^2+q^2u_F^2} . \quad (7)$$

Since at this frequency $\mathrm{Im}(\epsilon)$ also vanishes, $\Omega(q)$ is an exact zero of the complex Vlasov dispersion relation. It corresponds to the optical plasmon of a one-component equilibrium quantum plasma which is undamped at $T=0$ K (Fig. 2).

(ii) For an electron-ion plasma at $T=0$ K we set $i=2$ and consider equal Fermi momenta yielding for the velocities $u_{1e}=u_{1i}=0$, $u_{2e}=u_{2i}/\alpha=u_F$, where α denotes the mass ratio m_e/m_{ion}. There are now two undamped plasmons, given by

$$\Omega_{1,2}^2(q)=\frac{\omega_{pe}^2+q^2u_F^2}{2}\pm\frac{1}{2}\sqrt{\omega_{pe}^4+q^4u_F^4}+\frac{\alpha}{4}\left[2\omega_{pe}^2\pm\sqrt{\omega_{pe}^4+q^4u_F^4}\pm\frac{\omega_{pe}^4-q^4u_F^4-4q^2u_F^2\omega_{pe}^2}{\sqrt{\omega_{pe}^4+q^4u_F^4}}\right]+O(\alpha^2) . \quad (8)$$

Since $\mathrm{Im}(\epsilon)=0$ at these frequencies, $\Omega_{1,2}(q)$ are the well-known optical (+) and acoustic (−) plasmons of a two-component plasma. It is interesting to note that the undamping of the acoustic plasmon at zero temperature holds beyond the limits of the Vlasov theory.

(iii) The simplest model for a nonequilibrium distribu-

tion function is to set $i=2$, $u_1=0$, $u_2=u_F$, $u_{21}=u_3$, and $u_{22}=u_4$, $u_F<u_3<u_4$ in (4). This corresponds to nonequilibrium charge carriers with a background of equilibrium carriers at $T=0$ K. More realistic functions with smooth carrier distributions will be considered in Sec. VI. Avoiding here the lengthy analytic results for the plasmon dispersion, we mention only that there are three modes. The high frequency mode is undamped and corresponds again to the optical plasmon (mainly due to the nonequilibrium carriers). In addition, there are two complex conjugate solutions, corresponding to one damped ($\gamma>0$) and one growing ($\gamma<0$) mode.

Summarizing the dispersion results for distributions of the type (4), we find that the number of plasmon modes equals the number of boxes in the distribution function (including those at negative velocities). The modes are either exactly undamped or complex conjugate pairs. The real part of ϵ as a function of ω has zeros only at the plasmon modes. Due to the δ function shape of the imaginary part of ϵ the Vlasov theory yields no continua of pair excitations. These continua simply shrink to straight lines $\omega_{ij}(q)=qu_{ij}$, along which also the real part of ϵ diverges, jumping from plus to minus infinity. Hence, even in the long wavelength limit all quantum properties of the plasma are lost.

Generalized plasmon pole approximations for 1D plasmas

Besides the DF itself, we consider the spectral function

$$\Phi(q,\omega)=-\mathrm{Im}[1/\epsilon(q,\omega)] \tag{9}$$

(cf. Sec. III), which is important because it can be measured, for example, in inelastic polarized light scattering (Raman scattering) experiments (see, e.g., Ref. [35] for 3D systems, [36] for 2D quantum wells, and Ref. [27] for quantum wires). Calculating the spectral function for the systems under consideration first for finite temperatures and then for $T\to 0$ we find δ peaks at the positions of the plasmons. This implies that the Vlasov polarization (5) and (6) for the distribution functions (4) naturally generates plasmon pole approximations (cf. [2]). These are quite general, since we do not have to restrict the Coulomb potential to the 3D form (see Sec. III). For a one-component plasma, Eq. (5) can be written as a single-pole approximation,

$$\epsilon(q,\omega)=1-\frac{q^2V(q)n/m}{\omega^2-\Omega(q)^2+q^2V(q)n/m}\ , \tag{10}$$

where $\Omega(q)$ is given by (7). This formula can be applied to quantum wires also if the corresponding Coulomb potential and plasmon dispersion $\Omega(q)$ are used. Substituting $V(q)\to\omega_p^2 m/nq^2$ we get the result for 1D plasmas without quantum confinement.

The generalization to an s component plasma ($s=2,3,\ldots$) is straightforward.

III. DISPERSION RELATION FOR DEGENERATE PLASMAS

For the statistical description of collective excitations in quantum plasmas we have to use a quantum mechanical kinetic equation. The generalization of the Vlasov equation leads to the Hartree equation (collisionless Boltzmann equation) [37]. Linearizing this equation yields the RPA of the dielectric function which was given above by Eq. (2).

In the quantum case Π_a is the Lindhard polarization function [38] which in 1D is

$$\Pi_a(\omega,\gamma,q)=2\int_C\frac{dk}{2\pi}\frac{f_a(k)-f_a(k+q)}{E_a(k)-E_a(k+q)+(\omega-i\gamma)+i\delta}\ , \tag{11}$$

where δ is an infinitesimal small positive number. Here the normalization condition is $2\int(dk/2\pi)f_a(k)=n$, where n is the average 1D density, and $E_a(q)=\hbar^2q^2/2m_a$. $V(q)$ again is the matrix element of the Coulomb potential which depends on properties like band structure, dimensionality, and, in particular, on possible confinement effects. For example, in the case of quantum wires, where the carrier movement is confined to one direction, the Coulomb potential can be approximated by $V(q)=2e^2K_0(qd)/\epsilon_b$ [22,29]. Here K_0 denotes the Bessel function of second kind, ϵ_b is the background dielectric constant of the semiconductor material, and d is the width in the case of a plane wire. This Coulomb potential corresponds to the real space potential $V(x)=e^2/\epsilon_b(x^2+d^2)^{-1/2}$ [39]. To model a system of interacting quantum wires as well as for plasmas without quantum confinement one can use the 3D Coulomb potential $V(q)=4\pi e^2/q^2$.

Considering the Lindhard polarization (11), one can easily see that it reduces to the Vlasov polarization, (1), if q goes to zero, i.e., in the long wavelength limit. The Vlasov approach is not applicable if the wave vector is of the order of the characteristic width of the unperturbed distribution function (e.g., the Fermi momentum in low-temperature equilibrium plasmas). However, as we will show, even for small wave numbers the Vlasov theory yields only the "classical" properties of the plasma. Quantum effects, in particular the existence of a pair continuum and its properties, cannot be described by this approximation. Therefore a detailed investigation of the RPA dispersion relation is necessary. Generally, this is more difficult than the analysis of nondegenerate plasmas. First, because the derivative [in the numerator of Eq. (11)] is replaced by the difference of distribution functions, the integral becomes explicitly wave vector dependent. Therefore a multicomponent plasma cannot be reduced to a single-component one. Second, there are no such general and simple instability conditions such as, for example, the Penrose criterion [40].

An approximate solution of the RPA dispersion relation is possible if the damping [$\mathrm{Im}(\epsilon)$] is small. Then one can obtain the plasmon spectrum from $\mathrm{Re}(\epsilon)=0$ only [$\mathrm{Im}(\omega)=0$]. This is, however justified only at low temperatures, and may, moreover, lead to wrong results for the damping rates. The correct procedure is to carry out the analytic continuation of the retarded DF into the lower energy half plane. Therefore we calculate the integral in (11) according to Landau's prescription [7]. The result for the polarization function of a quasi-one-dimensional degenerate plasma is

$$\mathrm{Re}\Pi_a(\omega,\gamma,q)=\frac{m_a}{\pi q}\begin{cases}\int_{-\infty}^{\infty}dk\dfrac{[f_a(k+q)-f_a(k)][k-p_a^-]}{(k-p_a^-)^2+\delta_a^2}\ , & \gamma<0\\ P\int_{-\infty}^{\infty}dk\dfrac{f_a(k+q)-f_a(k)}{k-p_a^-}\ , & \gamma=0\\ \int_{-\infty}^{\infty}dk\dfrac{[f_a(k+q)-f_a(k)][k-p_a^-]}{(k-p_a^-)^2+\delta_a^2} & \\ -2\pi\,\mathrm{Im}[\tilde{f}_a(p_a^+-i\delta_a)-\tilde{f}_a(p_a^--i\delta_a)]\ , & \gamma>0\end{cases} \tag{12}$$

$$\mathrm{Im}\Pi_a(\omega,\gamma,q)=\frac{m_a}{\pi q}\begin{cases}-\delta_a\int_{-\infty}^{\infty}dk\dfrac{[f_a(k+q)-f_a(k)]}{(k-p_a^-)^2+\delta_a^2}\ , & \gamma<0\\ \pi[f_a(p_a^+)-f_a(p_a^-)]\ , & \gamma=0\\ -\delta_a\int_{-\infty}^{\infty}dk\dfrac{[f_a(k+q)-f_a(k)]}{(k-p_a^-)^2+\delta_a^2}+2\pi\,\mathrm{Re}[\tilde{f}_a(p_a^+-i\delta_a)-\tilde{f}_a(p_a^--i\delta_a)]\ , & \gamma>0\end{cases} \tag{13}$$

where we use $p_a^{\pm}=(m_a/q)[\omega\pm E_a(q)]$ and $\delta_a=\gamma m_a/q$. $\tilde{f}_a$ denotes the analytic continuation of the unperturbed distribution function into the lower half plane [41].

IV. PLASMONS IN ONE-COMPONENT EQUILIBRIUM PLASMAS

Let us consider first the case $T=0$ K. With the distribution function

$$f(k)=\Theta(k_F-|k|) \tag{14}$$

the Landau integration in (12) and (13) can be carried out analytically. For the analytical continuation of (14) we use

$$f(k)=\lim_{\Delta\to 0}F_\Delta(k)\ ,$$
$$F_\Delta(k)=\frac{1}{\pi}\left[\arctan\left[\frac{k+k_F}{\Delta}\right]-\arctan\left[\frac{k-k_F}{\Delta}\right]\right]\ . \tag{15}$$

For complex k, the arctan is a complex function. However, the imaginary part vanishes if Δ goes to zero and we can therefore drop it. The exact result for the real part of the equilibrium polarization function is

$$\mathrm{Re}\Pi(\omega,\gamma,q)=\frac{m}{2\pi q}\ln\frac{[\omega^2-\omega_2(q)^2]^2+2\gamma^2[\omega^2+\omega_2(q)^2]+\gamma^4}{[\omega^2-\omega_1(q)^2]^2+2\gamma^2[\omega^2+\omega_1(q)^2]+\gamma^4}\ , \tag{16}$$

$$\mathrm{Im}\Pi(\omega,\gamma,q)=\frac{m}{q}\begin{cases}F_\delta(p^+)-F_\delta(p^-)\ , & \gamma<0\\ F_\Delta(p^+)-F_\Delta(p^-)\ , & \gamma=0\\ F_\delta(p^+)-F_\delta(p^-)+2\,\mathrm{Re}[F_\Delta(p^+-i\delta)-F_\Delta(p^--i\delta)]\ , & \gamma>0\end{cases} \tag{17}$$

where we have used $p^{\pm}=(m/q)[\omega\pm E(q)]$, $\omega_{1,2}(q)=qk_F/m\pm E(q)$, $\delta=\gamma m/q$, and the limit $\Delta\to 0$ has to be taken. The $\Delta\to 0$ terms arise from the residia of the polarization function's denominator (11). This guarantees that $\mathrm{Im}\Pi$ will be continuous when it crosses the real frequency axis (notice $F_{-\alpha}=-F_\alpha$).

Using Eqs. (16) and (17) we can now simultaneously solve the equations $\mathrm{Re}(\epsilon)=0$ and $\mathrm{Im}(\epsilon)=0$ for the plasmon dispersion $\Omega(q)$ and damping $\Gamma(q)$. We will summarize the main results. First we find that $\mathrm{Re}(\epsilon)$ has singularities on the real frequency axis at the values $\omega_s(q)=|\omega_{1,2}(q)|$, which are the boundaries of the pair continuum. These lines include, for example, the $\omega=0$ divergencies at $q=0$ and $2k_F$, which are related to the Peierls instability [45]. For nonzero γ all singularities disappear, showing that plasmons are either damped or have a frequency different from ω_s. This can be seen in Fig. 1(a), where the zeros of the real part and the imaginary part of the DF in the complex frequency plane are shown. In our approach, collective plasma excitations are given by the crossing points of these lines. We see that the one-component equilibrium plasma has at zero temperature two clearly separated plasmons existing for all values of q. For a quantum confined plasma in a quantum wire both plasmon modes start at zero frequency [Figs. 1(c) and 1(d)]. In a 1D plasma without quantum confinement (3D Coulomb potential) the high frequency (optical) plasmon starts at the plasma frequency [line a in

Fig. 1(c)]. At zero temperature the (optical) plasmon is undamped, whereas the acoustic plasmon follows the upper edge of the continuum $\Omega_{ac}(q) \approx \omega_1(q)$ and is always damped. An important peculiarity of one-dimensional systems is the undamping region ($\mathrm{Im}\Pi = 0$) which is enclosed by the line $\omega_2(q)$ and the momentum axis [Fig. 1(b)] which occurs in 2D or 3D only in nonequilibrium.

From the DF we can now calculate the spectral function (9). It has a δ shaped peak at the frequency of the optical plasmon and a broader peak in the pair continuum with the maximum at the low frequency zero of $\mathrm{Re}(\epsilon)$, ($\mathrm{Im}\omega = 0$), cf. Fig. 3(a). Inelastic polarized light scattering experiments on quantum wire structures by Goñi *et al.* [27] have reproduced this result rather well. Their explanation of this continuum peak as "predominantly single-particle excitation" is based on similar Raman scattering results for 3D [35] and 2D [36]. For these systems this low frequency peak is usually assigned to single-particle excitations. Our results show that in the alternative description which uses the analytically continued DF this peak manifests itself in a zero of the DF with finite damping (even at $T = 0$ K). Thus in the density response of the plasma both zeros of the DF lead to macroscopic oscillations with their respectively frequency. There is no qualitative difference between them, they are distinguished only by the value of their damping [47]. However, for elevated temperatures or with carrier scattering taken into account, the damping rates become comparable (see below).

Let us now turn to equilibrium plasmas at finite temperature. The distribution function is the Fermi-Dirac function $f(k) = 1/\{\exp[\beta(k^2/2m - \mu)] + 1\}$, with β and $\mu = \mu(n, \beta)$ denoting the inverse temperature and the chemical potential, respectively. Due to the smooth edge of the Fermi function there is no undamping region at finite temperature, and the optical plasmon becomes damped as well. In Fig. 1(a) the zeros of the real and imaginary parts of the dielectric function are shown for $T = 100$ K. There are essential changes compared with the $T = 0$ K result, showing up as additional zeros of $\mathrm{Im}(\epsilon)$ and $\mathrm{Re}(\epsilon)$ which, however, lie at higher damping rates. The reason is the complicated pole structure of the analytic continuation of the Fermi function [41]. These poles are located at the Matsubara frequencies. In their vicinity they perturb the surface of the polarization function in the complex frequency plane. While these disturbances vanish at zero temperature, for increasing T the poles depart from the real frequency axis and their influence grows. The effect of temperature on the plasmon dispersion is shown in Fig. 2, where the two complex zeros of the DF, corresponding to the $T = 0$ K result, are shown for different temperatures. With in-

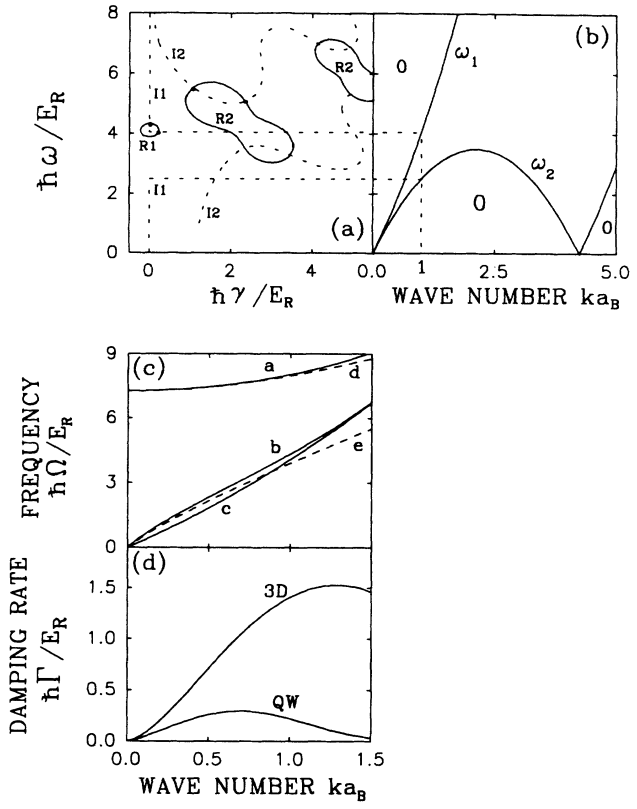

FIG. 1. Collective excitations of an electron plasma in equilibrium (GaAs: $\epsilon_b = 12.7$, $a_B = 135$ Å, $E_R = 4.2$ meV). (a) Zeros of the analytic continuation of the retarded RPA dielectric function (DF) for $k = 1/a_B$. Plasmons (marked by thick dots) correspond to the crossing of the lines $\mathrm{Re}(\epsilon) = 0$ ($R1$ for $T = 0$ K and $R2$ for $T = 100$ K, respectively) and $\mathrm{Im}(\epsilon) = 0$ ($I1$ and $I2$ for $T = 0$ and 100 K, respectively). (b) Pair continuum and undamping regions ("0") ($\gamma = 0$ and $T = 0$ K), $\omega_{1,2} = q/2m(2k_F \pm q)$. (c) Plasmon dispersion at $T = 0$ K, $n = 10^6$ cm^{-1}. The optical mode is shown for the 3D Coulomb potential (*a*) and the case of a quantum wire (*b*) of thickness $d = 2/3a_B$, respectively. *c* is the acoustic mode (both cases), *d* and *e* are extrapolations from the Vlasov DF. (d) Damping rate of the acoustic plasmon for the 3D Coulomb potential and the quantum wire potential (QW).

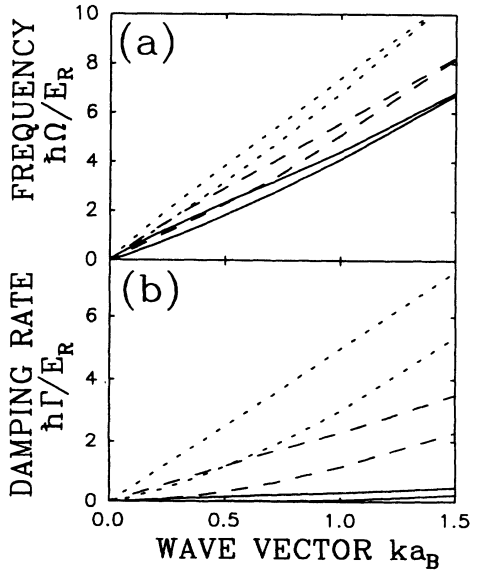

FIG. 2. Plasmons in the quantum wire of Fig. 1 at $T = 10$ K (full line), $T = 100$ K (long-dashed line), and $T = 300$ K (short-dashed line). (a) Plasmon dispersion, (b) damping rates.

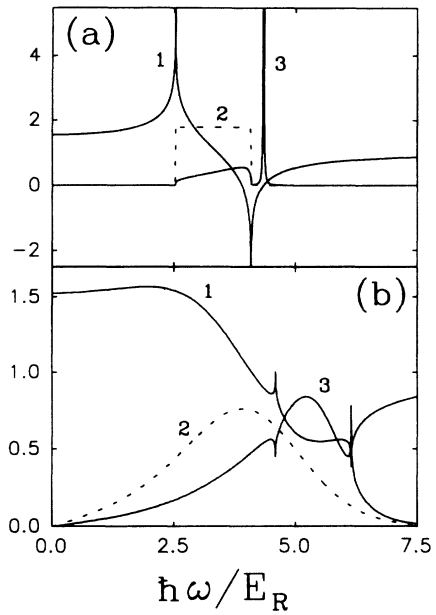

FIG. 3. Real (1) and imaginary (2) part of the DF, and spectral function (3) for an electron plasma at $T=0$ K (a) and $T=100$ K (b), corresponding to the quantum wire in Fig. 1. $\gamma=0$, $k=1/a_B$, $n=10^6$ cm^{-1}.

creasing temperature the frequencies of all plasmons shift upwards. This is due to the fact that plasma oscillations are now excited in a medium of faster moving particles. This leads to an increase of the screening length r. Similar results have been found in 2D and 3D plasmas, which can be seen, e.g., from the small q limit. There one can write for the frequency of the optical plasmon $\Omega^2(q)=\omega_p^2[1+\alpha(q,n,T)]$, with $\alpha^{3D}=q^2r_{3D}^2$ and $\alpha^{2D}=qr_{2D}$, e.g., [3]. However, there is an even stronger increase of the Landau damping of the oscillations.

Notice that, as in 3D, there exists a critical momentum $q_{cr}(T)$, beyond which $\mathrm{Re}(\epsilon)$ no longer has zeros at $\gamma=0$ [Fig. 3(b)]. Nevertheless, there are still complex zeros of the dielectric function at positive γ [see Fig. 1(a)], which can be resolved in the spectral function. Their association with resonances [2] or with damped collective excitations is a question of interpretation.

V. PLASMONS IN TWO-COMPONENT EQUILIBRIUM PLASMAS

We now consider the case of two species of charge carriers, electrons (e) and positive charges (p: holes, protons, or positively charged ions). Electroneutrality is assumed, therefore, in the case of single charged ions, the densities are equal, $n_e=n_p$. Let us again start with the case $T=0$ K. The distribution function for both species is given by (14) where we choose the same values for the Fermi momenta. The result for the polarization function is Eqs. (16) and (17). The only difference is that the mass m has to be replaced by m_e or m_p. Correspondingly, the DF is given by Eq. (2). Figure 4 shows the overlapping pair continua for the case of an electron-hole plasma. Considering the plasmons, one finds that at $T=0$ K both components behave nearly independently, each component

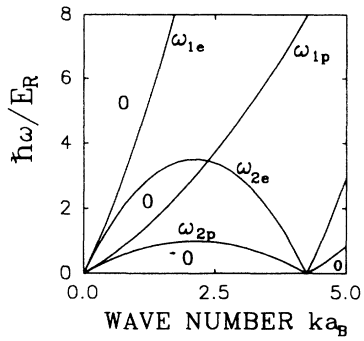

FIG. 4. Same as Fig. 1(b), but for a two-component plasma at $T=0$ K. Indexes e and p correspond to electrons and positive carriers, respectively.

exhibiting two plasmons. Compared with the single-component case we observe a minor increase (decrease) of the frequency of the optical plasmon as well as slightly stronger (weaker) damping of the acoustical one for the lighter (heavier) species. The unexpected result is that even the heavy component has an undamped plasmon [46] which is due to the overlap of the undamping regions of both components. (In the case of the Vlasov dispersion this was not surprising due to the vanishing of the pair continuum.) Only for momenta between $2k_F(m_p-m_e)/(m_p+m_e)$ and $2k_F(m_p+m_e)/(m_p-m_e)$, where both continua overlap, are there no collective excitations of the heavy species. For ionized gases where the positive carriers are at least three orders of magnitude heavier than the electrons this overlap region is negligibly small. However, if the mass of the positive carriers approaches that of the electrons, the overlap region covers the whole interval $[0,2k_F]$, so that in the limit of equal masses (such as, e.g., for electron-positron plasmas) only one undamped plasmon remains (which is twofold degenerate). Figure 5 illustrates the scaling of frequencies and wave numbers of the two undamped plasmons for different two-component quasi-1D plasmas: An

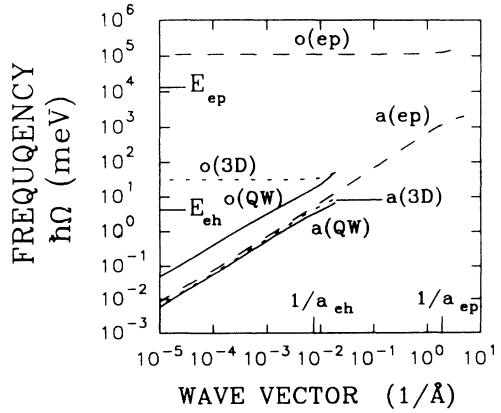

FIG. 5. Dispersion of the undamped plasmons in a two-component 1D quantum plasma at $T=0$ K. The case of an electron-hole (eh) plasma with (QW) and without (3D, dotted lines) quantum confinement as well as an electron-proton (ep, dashed lines) plasma are shown. $T=0$ K, $n=10^6$ cm^{-1}. o denotes the optical and a the acoustic plasmon. $E_{ep}=13.6$ eV and $E_{eh}=4.2$ meV are the binding energies.

electron-hole plasma (GaAs) with and without quantum confinement and an electron-proton plasma [48].

For the case of finite temperatures, with Fermi distributions of both components, the interesting point is that with increasing temperature the overlap of both continua is getting stronger, and both components lose their independent character. The undamped oscillation of the heavy species ($T=0$ K) becomes damped too. But this damping is only of the same order as that of the corresponding optical electron mode.

VI. PLASMONS IN NONEQUILIBRIUM PLASMAS

We will now consider nonequilibrium situations, where in addition to thermal carriers the system contains a portion of nonequilibrium (fast) carriers. In the limit where the momentum of both fractions has sharp boundaries, we can expect that the fast carriers act like an independent second component. The opposite situation corresponds to distribution functions with two overlapping maxima. Let us start with the first case, which is described by the distribution function (4) and for which the polarization function can be found analytically. For the analytic continuation we consider the generalization of (15):

$$f_a(k)=\lim_{\Delta\to 0}\sum_i A_{ai}F_\Delta^{(ai)}(k)\ ,$$
$$F_\Delta^{(ai)}(k)=F_\Delta^{(ai)+}(k)+F_\Delta^{(ai)-}(k)\ , \tag{18}$$
$$F_\Delta^{(ai)\pm}(k)=\pm\frac{1}{\pi}\left[\arctan\left[\frac{k\pm k_1^{(ai)}}{\Delta}\right]-\arctan\left[\frac{k\pm k_2^{(ai)}}{\Delta}\right]\right]\ .$$

The exact result for the real part of the polarization function is

$$\mathrm{Re}\Pi_a(\omega,\gamma,q)=\frac{m_a}{2\pi q}\ln\prod_i\left[\frac{S_a(\omega,\gamma,q;k_2^{(ai)})}{S_a(\omega,\gamma,q;k_1^{(ai)})}\right]^{A_{ai}}\ ,$$
$$S_a(\omega,\gamma,q;k)=\frac{P_{a-}^2(\omega^2,\gamma^2,q;k)}{P_{a+}^2(\omega^2,\gamma^2,q;k)}\ , \tag{19}$$
$$P_{a\pm}^2(\omega^2,\gamma^2,q;k)=[\omega^2-\omega_{a1,2}^2]^2+2\gamma^2[\omega^2+\omega_{a1,2}^2]+\gamma^4\ ,$$

where $\omega_{a1,2}=qk/m_a\pm E_a(q)$. The imaginary part of the polarization is

$$\mathrm{Im}\Pi_a(\omega,\gamma,q)=\frac{m_a}{q}\sum_i A_{ai}\begin{cases}F_{\delta_a}^{(ai)}(p_a^+)-F_{\delta_a}^{(ai)}(p_a^-)\ , & \gamma<0\\ F_\Delta^{(ai)}(p_a^+)-F_\Delta^{(ai)}(p_a^-)\ , & \gamma=0\\ F_{\delta_a}^{(ai)}(p_a^+)-F_{\delta_a}^{(ai)}(p_a^-)+2[\mathrm{Re}F_\Delta^{(ai)}(p_a^+-i\delta_a)-\mathrm{Re}F_\Delta^{(ai)}(p_a^--i\delta_a)]\ , & \gamma>0\ .\end{cases} \tag{20}$$

The dispersion analysis shows that the number of solutions (modes) with positive frequency equals $2KN$, where K is the number of components and N the number of maxima of the distribution function (4), including those at negative momenta. Unstable modes are always accompanied by a complex conjugate (damped) mode. This result agrees with that for the corresponding Vlasov dispersion relation (Sec. II), except that there are now twice as many solutions. Each "Vlasov plasmon" is here accompanied by an acoustic mode of the same type as the one-component equilibrium case (Sec. IV).

For the distribution (4), case (iii), the dispersion relation yields six collective modes, as can be seen from the behavior of the DF [Fig. 6(b)]. The high frequency pair (I,II) is similar to equilibrium plasmons having frequencies close to the upper edge of the continuum [$\Omega(q)=E(q)+qk_4/m$]. Modes IV,V are the unstable plasmon and its complex conjugate counterpart. These modes are surrounded by two damped plasmons (III,VI) which follow the edges of the undamping ($\mathrm{Im}\Pi=0$) region with the dispersions $\Omega_{\mathrm{VI}}(q)\approx E(q)+qk_F/m$ and $\Omega_{\mathrm{III}}(q)\approx qk_3/m-E(q)$. The corresponding wave vector dispersion of the modes for the quantum wire was given in [20].

The determination of the necessary and sufficient conditions for unstable plasmons in degenerate plasmas is more complicated than for classical systems, since, e.g., the Penrose criterion [40] is not applicable. One useful tool to check for the existence of unstable modes is the Nyquist diagram [49]. The necessary condition for the existence of an instability is a minimum of the distribution function leading to a damping inversion region [$\mathrm{Im}\Pi>0$, see Fig. 6(a)]. But this allows an instability only if the interaction between the thermal and the fast carriers is strong enough so that an energy transfer can occur. In Fig. 6(b) one can see that a complex zero at the DF at negative "damping" (point IV) exists only if there is an overlap of the lines $\mathrm{Re}(\epsilon)=0$ corresponding to the thermal and the hot carriers, respectively. Otherwise the real part of the DF has two zeros on the real frequency axis between $\Omega_{\mathrm{III}}(q)$ and $\Omega_{\mathrm{VI}}(q)$, leading to a pair of undamped plasmons instead of the complex conjugate pair. These plasmons cause a pair of δ shaped peaks in the spectral function.

Above a critical value q_{cr} the instability disappears. In [20] it was pointed out that the following factors act in favor of the instability: high density of the fast carriers, a small gap between the equilibrium and the nonequilibrium peak, and a strong Coulomb potential. Large growth rates should occur for the 3D Coulomb potential. For

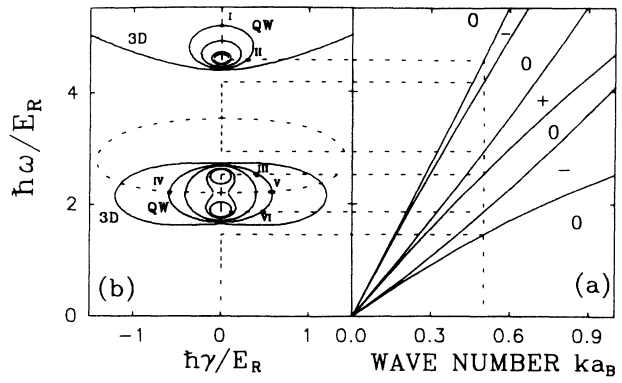

FIG. 6. Dispersion analysis for a nonequilibrium electron plasma with the distribution function Eq. (4), case (iii), $k_F=2.12$, $k_3=3.5$, $k_4=k_3+k_F$. (a) Pair continua, undamping and inversion ($\mathrm{Im}\Pi>0$) regions (signs indicate the signs of $\mathrm{Im}\Pi$, $\gamma=0$, $q=0.5/a_B$). $\omega_{1,2}=q/2m(2k_F\pm q)$, $\omega'_{1,2}=q/2m(2k_3\pm q)$, $\omega''_{1,2}=q/2m(2k_4\pm q)$. (b) Zeros of the real part (full lines) and of the imaginary part (dotted lines) of the DF for a quantum wire of width (in Bohr radii) 0.5, 1, 1.5, and 2 (from large to small ellipses) and the 3D Coulomb potential, respectively. Plasmons are marked with dots (for the first case only).

quantum confined systems the Coulomb potential is weaker, in particular, the instability will disappear above a critical wire width. Figure 7 shows the dispersion and growth rate of the unstable mode for both cases of the Coulomb potential. The most interesting result is the almost linear dispersion of the unstable mode which can be

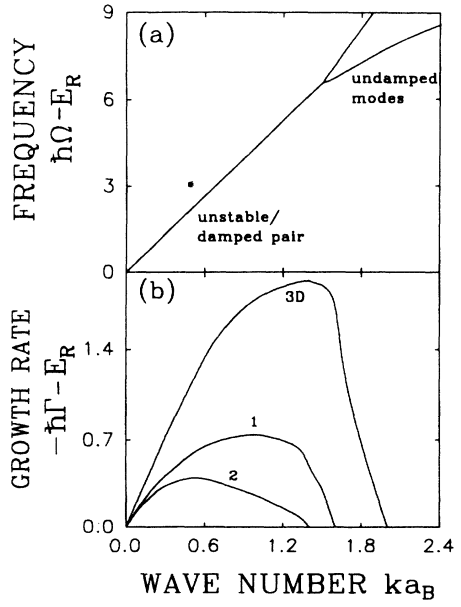

FIG. 7. Dispersion of the complex conjugate mode pair of the system of Fig. 6 for a quantum wire potential. (a) Dispersion of the unstable-stable pair for a wire of $d=0.5a_B$. Above a critical wave number these modes are replaced by a pair of undamped modes. (b) Growth rate of the unstable mode. (1) and (2) correspond to a quantum wire of thickness $0.5a_B$ and $1a_B$, respectively, and 3D corresponds to the 3D Coulomb potential.

well approximated by

$$\Omega_{\mathrm{inst}}(q)=(k_F+k_3)q/m\ , \tag{21}$$

allowing us to speak about a carrier-acoustic instability [20,21].

There are other factors which will decrease the growth rates or limit the instability to lower q values: carrier-carrier and carrier-phonon scattering, which will be discussed in Sec. VII. Since temperature increase leads to increased damping of plasmons in equilibrium, cf. Figs. 1(a) and 2, we have to expect the same effect in nonequilibrium. The result is shown in Fig. 8.

In order to answer the question of how the instability depends on the shape of the distribution of the nonequilibrium carriers we consider a Gaussian with the same particle number, centered at the same momentum as the above box function:

$$f_N(k)=A_N\{\exp[-(k-k_0)^2/2\Delta] +\exp[-(k+k_0)^2/2\Delta]\}\ . \tag{22}$$

The results for the unstable mode for temperatures between 0 and 200 K are shown in Fig. 8. Increasing the temperature causes a less pronounced minimum of the distribution function which limits the instability to smaller values of the wave number and decreases the growth rate. Therefore it is plausible that the best developed instability occurs if the carrier distribution has sharp boundaries as in the case of Eq. (4). Variation of the parameters, in particular the wire width, should allow one to increase the critical momentum and the growth rates further. It is interesting to note that although the growth rate of the unstable mode strongly depends on the shape of the nonequilibrium distribution function, the dispersion remains nearly the same as in the model case of two boxes, given by (4).

In the case of a two-component nonequilibrium plasma the analysis can be done in the same way. One finds possibly two unstable modes, one for each component.

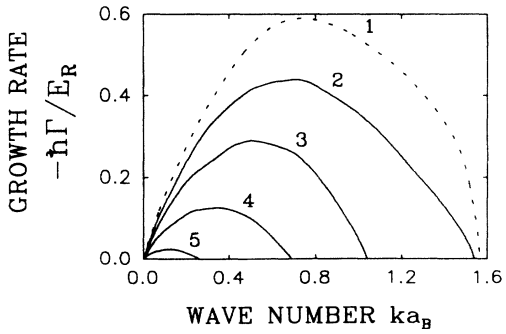

FIG. 8. Growth rates for the unstable mode for different nonequilibrium distributions and different temperatures. The dotted (1) line corresponds to a nonequilibrium box ($k_3=3.5$, $k_4=5.62$) with a background plasma at $T=0$ K. Solid lines show the result for a Gaussian distribution, Eq. (22) ($A_N=1$, $x_0=4.56$, $\Delta=0.72$), with a background plasma at $T=0$ K (2), $T=50$ K (3), $T=100$ K (4), and $T=200$ K (5). The equilibrium and nonequilibrium densities are in all cases both equal to 10^6 cm^{-1}.

VII. LIMITATIONS OF THE RPA

Assuming the Coulomb interaction is small compared to the kinetic energy, the RPA is valid only outside the "corner of correlations" mentioned in Sec. I. For degenerate plasmas this implies electron densities $na_B > 1$. For gaseous plasmas this condition can be satisfied only under high pressure conditions like those mentioned in Sec. I [56], whereas for plasmas in solids it leads to reasonable parameters. For quasi-one-dimensional semiconductor quantum wires it was shown that the RPA does not lead to intrinsic contradictions if the electron density exceeds the inverse exciton Bohr radius at least by a factor of 1.5 [33]. (This corresponds to densities above 10^6 cm^{-1}). Our calculations are close to these values. In general, one has to check the importance of effects beyond the RPA, in particular carrier-carrier and carrier-phonon scattering. As long as the characteristic scattering times exceed the inverse damping or growth rates, these effects can usually be neglected. This condition is fulfilled in quasi-1D systems much better than in 2D or even 3D, especially in quantum confined plasmas. Due to energy and momentum conservation electron-electron scattering does not contribute to the relaxation to equilibrium. Even if the spin splitting of the conduction band is taken into consideration, the scattering rates remain very low [52]. The influence of carrier-carrier and carrier-phonon scattering on the behavior of 1D plasmas was investigated recently in time resolved luminescence experiments [26]. Furthermore, Monte Carlo simulations have been carried out [53]. Both suggest that the scattering rates are reduced essentially in comparison to the bulk case [54], leading to relaxation times τ exceeding one picosecond. Based on these results one can use a relaxation time approximation to include collision effects into the DF [34]:

$$\Pi(q,\omega)=\Pi^0(q,0)\frac{(1+i/\omega\tau)\Pi^0(q,\omega+i/\tau)}{\Pi^0(q,0)+i/\omega\tau\Pi^0(q,\omega+i/\tau)} . \quad (23)$$

Here Π^0 is the RPA polarization calculated without taking collisions into account. The total damping is, in this approximation, given by the sum of Landau damping and collisional damping. In the case of instabilities the collision effects tend to lower the growth rates (i.e., suppress the instability). The result will be a shift of the critical wave number $q_{cr}(T;V(q))$ to lower values, or, in the case of quantum wires, the limitation of the instability to thinner structures.

The second problem with the RPA is that it yields only exponentially (Landau) damped or growing modes. Especially in the case of instabilities this theory can therefore be used only on short time scales (i.e., as long as the plasmon energy remains small compared to the thermal energy). Based on our calculated growth rates, one can easily calculate the time after which the field energy will reach the order of the mean kinetic energy. The minimum of this time and the relaxation time defines then the time interval for which the RPA result is appropriate. In the systems under consideration this time is expected to be of the order of several picoseconds. However, the validity of the RPA for small amplitude oscillations is also not trivial. In particular, for nonequilibrium distributions with several extrema not all assumptions necessary for the linearization are fulfilled ($|\partial f_1/\partial p|$ is not everywhere small compared to $|\partial f_0/\partial p|$). Therefore we solved the full nonlinear collisionless Boltzmann equation numerically. The result for the density evolution corresponding to an unstable situation with the distribution function of Eq. (22) added to a Fermi function is shown in Fig. 9. One can see that for small amplitude oscillations the agreement with the RPA result is very good. Also, the frequency of the unstable mode derived from the RPA was reproduced with an error of less than 1%. Details of the numerical solution and additional results will be given in [55].

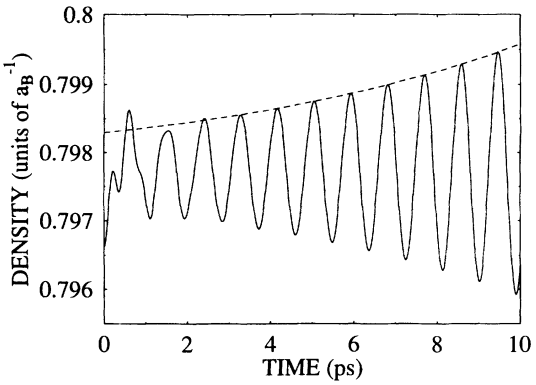

FIG. 9. Local carrier density calculated using the nonlinear collisionless kinetic equation (full line) compared with the exponential growth rate determined from the complex zeros of the RPA DF (dashed line). After the optical plasmon's decay, growth of the unstable mode closely matches that predicted by the RPA. The distribution of the nonequilibrium carriers is a Gaussian, cf. Eq. (22), $A_N=0.7$, $k_0=1.5$, $\Delta=0.101$, the temperature and the density of the background plasma are $T=5$ K, and $n=0.44/a_B$.

VIII. CONCLUSIONS

The equilibrium and nonequilibrium plasmons in degenerate quasi-1D plasmas have been studied within the random-phase approximation, generalizing the classical results from the Vlasov theory. Our analysis focused on the common features of 1D quantum plasmas, including gases, metals, organics, and plasmas in quantum wires. The main differences between these systems are different forms of the Coulomb potential. Nevertheless, the results obtained for one particular system can easily be transferred to another one, by rescaling the frequencies, the wave number (i.e., the Rydberg energy and the Bohr radius, respectively), and the effective mass (Fig. 5). We have shown that the Vlasov theory applied to zero-temperature distribution functions directly yields generalized plasmon pole approximations, which can be useful in complex calculations. The results of the Vlasov dispersion are of interest for classical plasmas but also for degenerate systems in the long wavelength limit. However, it was shown that generally the Vlasov dispersion neglects all specific quantum effects (such as the pair con-

tinuum, single-particle excitations, and corresponding details of the spectral function).

For this reason it was necessary to consider the quantum generalization of the Vlasov DF, given by Lindhard (RPA). Applying the complex integration method proposed by Landau we calculated the 1D DF for arbitrary distribution functions and for arbitrary damping. For zero temperature and for several limiting cases of the nonequilibrium distributions the results could be obtained analytically. This allowed us to calculate the complete excitation spectrum and the correct damping of the plasmons. For many-component plasmas at $T=0$ K we found an undamped plasmon mode for each of the species.

Considering nonequilibrium plasmas we specified conditions for the existence of unstable modes in 1D plasmas. Of special interest for plasmas in semiconductor quantum wires is the dependence of the instability on the wire width. In order to verify that our results are not only a special feature of the RPA at zero temperature, we performed calculations for temperatures up to room temperature and we studied the influence of collisions and of the nonlinear terms in the Hartree equation.

ACKNOWLEDGMENTS

This work was supported by grants from the NSF, ARO/AFOSR(JSOP), NEDO, OCC, Deutsche Forschungsgemeinschaft, and grants for CPU time at the Pittsburgh Supercomputer Center and the University of Arizona's Center for Computing and Information Technology. M.B. acknowledges financial support by the Deutscher Akademischer Austauschdienst.

[1] See, e.g., *Strongly Coupled Plasma Physics,* edited by H. M. Van Horn and S. Ichimaru (University of Rochester Press, Rochester, 1993).

[2] See, e.g., W.-D. Kraeft, D. Kremp, W. Ebeling, and G. Röpke, *Quantum Statistics of Charged Particle Systems* (Akademie-Verlag, Berlin, 1986).

[3] H. Haug and S. W. Koch, *Quantum Theory of the Optical and Electronic Properties of Semiconductors,* 2nd ed. (World Scientific, Singapore, 1993).

[4] D. Kremp, M. Schlanges, M. Bonitz, and T. Bornath, Phys. Fluids B **5**, 216 (1993).

[5] A. A. Vlasov, Zh. Eksp. Teor. Fiz. **8**, 291 (1937). See, e.g., A. A. Vlasov, *Many-Particle Theory and Its Application to Plasma* (Gordon and Breach, New York, 1961).

[6] A. A. Vlasov, J. Phys. (Moscow) **9**, 25 (1945).

[7] L. D. Landau, J. Phys. (Moscow) **10**, 25 (1946).

[8] B. B. Kadomtsev, *Plasma Turbulence* (Academic, New York, 1968).

[9] A. B. Mikhailovski, *Theory of Plasma Instabilities* (Atomizdat, Moscow, 1975).

[10] G. Ecker, *The Theory of Fully Ionized Plasmas* (Academic, New York, 1972).

[11] R. C. Davidson, in *Handbook of Plasma Physics,* edited by M. N. Rosenbluth and R. Z. Sagdeev (Elsevier, Amsterdam, 1983).

[12] P. Gluck, Nuovo Cimento **38**, 67 (1971).

[13] Yu. L. Klimontovich and W. D. Kraeft, Teplofiz. Vys. Temp. **12**, 239 (1974) [High Temp. (USSR) **12**, 212 (1974)].

[14] D. Bohm and D. Pines, Phys. Rev. **92**, 3 (1953).

[15] D. Pines and J. R. Schrieffer, Phys. Rev. **124**, 1387 (1961).

[16] J. Pozhela, *Plasma and Current Instabilities in Semiconductors* (Pergamon, New York, 1981).

[17] E. ElSayed, R. Binder, D. C. Scott, and S. W. Koch, Phys. Rev. B **47**, 16 (1993).

[18] P. Bakshi, J. Cen, and K. Kempa, J. Appl. Phys. **64**, 2243 (1988).

[19] K. Kempa, P. Bakshi, and H. Xie, Phys. Rev. B **48**, 9158 (1993).

[20] M. Bonitz, R. Binder, and S. W. Koch, Phys. Rev. Lett. **70**, 3788 (1993).

[21] P. Bakshi, J. Cen, and K. Kempa, Solid State Commun. **76**, 835 (1990).

[22] I. E. Dzyaloshinskii and E. I. Kats, Zh. Eksp. Teor. Fiz. **55**, 338 (1968) [Sov. Phys. JETP **28**, 178 (1969)].

[23] J. Ruvalds, F. Bosens, L. F. Lemmens, and J. T. Devreese, Solid State Commun. **23**, 243 (1977).

[24] P. F. Williams and Aaron N. Bloch, Phys. Rev. B **10**, 1097 (1974).

[25] *Theoretical Aspects of Band Structures and Electronic Properties of Pseudo-One-Dimensional Solids,* edited by H. Kamimura (Reidel, Boston, 1985); *Electronic Properties of Inorganic Quasi-One-Dimensional Compounds,* edited by P. Monceau (Reidel, Boston, 1985); S. Kagoshima, H. Nagasawa, and T. Sambongi, *One-Dimensional Conductors* (Springer-Verlag, Berlin, 1988).

[26] R. Cingolani, H. Lage, H. Kalt, D. Heitmann, and K. Ploog, Phys. Rev. Lett. **67**, 891 (1991).

[27] A. R. Goñi, A. Pinczuk, J. S. Weiner, J. M. Calleja, B. S. Dennis, L. N. Pfeiffer, and K. W. West, Phys. Rev. Lett. **67**, 3298 (1991).

[28] T. Demel, D. Heitmann, P. Grambow, and K. Ploog, Phys. Rev. Lett. **66**, 2657 (1991).

[29] S. Das Sarma and Wuyan Lai, Phys. Rev. B **32**, 1401 (1985).

[30] Q. P. Li and S. Das Sarma, Phys. Rev. B **43**, 11 768 (1991).

[31] A. Gold and A. Ghazali, Phys. Rev. B **41**, 7626 (1990).

[32] A. Gold, Z. Phys. B **89**, 213 (1992).

[33] S. Benner and H. Haug, Z. Phys. B **84**, 81 (1991).

[34] N. D. Mermin, Phys. Rev. B **1**, 2362 (1970).

[35] A. Pinczuk, L. Brillson, E. Burstein, and E. Anastassakis, Phys. Rev. Lett. **27**, 317 (1971).

[36] D. Richards, B. Jusserand, H. Peric, and B. Etienne, Phys. Rev. B **47**, 16 028 (1993).

[37] L. P. Kadanoff and G. Baym, *Quantum Statistical Mechanics,* 2nd ed. (Addison-Wesley, Reading, MA, 1989).

[38] J. Lindhard, K. Dan. Vidensk. Selsk. Mat. Fys. Medd. **28**, 8 (1954).

[39] The real space Coulomb potential can also be well approximated by $V(x)=e^2/\epsilon_b(|x|+\gamma R)^{-1}$, where R is the radius in the case of a cylindrical wire and the fitting parameter $\gamma \approx 0.3$ [3].

[40] O. Penrose, Phys. Fluids **3**, 258 (1960).

[41] Note that $\tilde{f}_a$ can have poles itself. But, since the original distribution function is assumed to have no poles we have to choose the complex integration contour such that it avoids the poles of $\tilde{f}_a$. Nevertheless, these poles show up very pronounced in the dispersion, and may cause even additional zeros of the complex DF, as can be seen from

Fig. 1(a). Lying at higher damping rates than the collective excitations, these additional poles will, however, not influence the long-time behavior of the plasma essentially. These questions have been discussed extensively in the context of Vlasov plasmas [42–44].

[42] J. N. Hayes, Nuovo Cimento **30**, 1048 (1963).

[43] J. Denavit, Phys. Fluids **8**, 471 (1965).

[44] A. W. Saenz, J. Math. Phys. **6**, 859 (1965).

[45] R. E. Peierls, *Quantum Theory of Solids* (Oxford University Press, London, 1955).

[46] This fact was noticed also in Ref. [27] for the case of a quantum wire.

[47] Note, however, that in the usual notation the plasmon width is determined by the broadening of the one-particle states (which is zero in our RPA consideration), whereas our "acoustic plasmon" width is, analogously to inhomogeneous line broadening, determined by the spectral overlap of a continuum of single-particle excitations.

[48] For hydrogen at $T=0$ K this is of course only a qualitative calculation which neglects the influence of atoms and molecules on the dispersion.

[49] Plotting imaginary part of the DF versus real part, for ω going from minus infinity to plus infinity, at zero damping. (The Nyquist diagram allows one to determine the number of unstable plasmons in the system. This method is originally due to Nyquist [50] and will be applied to degenerate plasmas in [51]).

[50] H. Nyquist, Bell Syst. Tech. J. **11**, 126 (1932).

[51] D. C. Scott, R. Binder, M. Bonitz, and S. W. Koch, Phys. Rev. B **49**, 2174 (1993).

[52] G. Fasol and H. Sakaki, Phys. Rev. Lett. **70**, 3643 (1993).

[53] L. Rota, F. Rossi, S. M. Goodnick, P. Lugli, E. Molinari, and W. Porod, Phys. Rev. B **47**, 1632 (1993).

[54] D. C. Scott, R. Binder, and S. W. Koch, Phys. Rev. Lett. **69**, 347 (1992).

[55] D. C. Scott, R. Binder, M. Bonitz, and S. W. Koch (unpublished).

[56] Note that for the situation in gaseous plasmas one has to rescale the temperature by the ratio of the binding energies (for hydrogen $E_H/E_{ex} \approx 3200$).